Image Blur Assessment with Feature Points

Hao Cai, Leida Li* and Jiansheng Qian

School of Information and Electrical Engineering
China University of Mining and Technology
Xuzhou, 221116, China
*Corresponding author: lileida@cumt.edu.cn

Jeng-Shyang Pan

College of Information Science and Engineering
Fujian University of Technology
Fuzhou City, Fujian Province, China
Department of Computer Science and Technology
Harbin Institute of Technology Shenzhen Graduate School
Shenzhen, 518055, China

ABSTRACT. *Blur is a key factor in the perception of image quality, leading to spread of edges in images. The quantity of feature points extracted from images can represent image shape changes. Compared with sharp images, blurred images tend to contain less feature points, and the reduction of feature points is related to blur. In this paper, we propose a new blind blur assessment metric based on feature points. First, we apply Gaussian blur to the blurred image, producing the re-blurred image. Then feature points from the blurred and re-blurred images are extracted and used to form feature point maps. Next, each feature point map is divided into blocks to compute block-wise quantity map, based on which a feature point similarity map is calculated. Finally, a visual saliency map is employed to conduct the pooling, producing the final blur score. Experimental results on four public databases demonstrate that the predicted blur scores has high correlation with subjective evaluations, and the proposed method outperforms several no-reference image blur metrics, as well as some representative general-purpose blind image quality metrics.*
Keywords: Image quality assessment, No-reference, Blur, Feature points, Visual saliency.

1. **Introduction.** The processing and transmission of digital images usually lead to degraded visual quality. The subjective evaluation is time-consuming and difficult to implement in real world applications. Hence, we require objective image quality assessment (IQA) algorithms that can measure image quality, and the objective assessment results need to keep consistent with the human visual system (HVS). IQA aims at evaluating the quality of an image in an automatic and perceptually consistent way.

The current objective IQA methods can be classified into full-reference (FR), reduced-reference (RR) and no-reference (NR) metrics [1]. For FR metrics, the quality of a distorted image is evaluated with full access to the undistorted reference image [2]. Instead of using the whole reference image, RR metrics only use partial information of it [3]. However, in many practical application, the partial/full information about the reference image is inaccessible. Therefore, NR metrics that can predict the image quality only using the distorted image are comparatively more desirable. The NR metrics can be further classified into two types, namely distortion-specific metrics and general-purpose metrics.

While the former evaluates a specific kind of distortion, such as blocking artifacts [4, 5, 6], blur [7, 8] and ring artifacts [9], the latter estimates the quality of an image without knowing the exact distortion types [10]. In this paper, we focus on the NR image blur assessment.

In recent years, several algorithms have been proposed for image blur assessment. Marziliano et al. [11] detected image edges through the Sobel operator. Then the spread of edges was measured by the widths of the edges and blur score was computed as the average edge width. Shaked et al. [12] utilized localized frequency content analysis in a feature-based context, which facilitated automatic image blur enhancement. Ferzli et al. [13] proposed a sharpness metric by measuring curve variation of the image in the Riemannian manifold and mapping the image into a non-Euclidean space. The same authors [7] also proposed the concept of Just Noticeable Blur (JNB). Based on the local contrast and edge width of blocks, the image blur was modeled by a probabilistic framework. In [14], a NR metric (Q-metric) was proposed based on the singular value decomposition, and the gradients of local image anisotropic patches was calculated.

Blur is typically characterized by the spread of edges in images. Feature point detection is an important procedure in many computer vision applications, which is sensitive to image shape changes. Generally, more feature points can be extracted from a sharp image than a blurred counterpart, and the reduction of feature points is related to blur. Besides, the variation of feature points has correlation with geometric structures of image pixels. Hence, we can evaluate blur extent through the reduction speed of feature points combined with proper content-based pooling.

Based on this observation, this paper presents a new NR blur assessment method based on feature points. In order to evaluate the blur extent, we use the idea of relative blur. Therefore, we first apply Gaussian blur to the blurred image and obtain the re-blurred image. Then feature points of both the blurred and re-blurred images are extracted using the Harris corner detector [15], and the extracted feature points form a feature point map. Next, the feature point maps are divided into blocks to compute block-wise quantity maps, respectively. Later, a feature point similarity map is calculated based on the block-wise quantity maps. Finally, an overall blur score is produced by pooling this similarity map with a visual saliency map, which is mainly incorporated to adapt to the characteristics of the HVS.

2. **Harris Corner Detector.** The Harris corner detector [15] has been widely used in literature. The idea of Harris corner detector is to detect corner points (i.e., feature points), which are chosen by the local maxima of corner strength map based on the auto-correlation matrix of image gradients. In implementation, the Harris corners are detected following four steps. First, an image is filtered by Gaussian filter to obtain directional derivative distorted images I_m and I_n. Second, eigenvalues or the autocorrelation matrix M are computed in a Gaussian window W around each pixel. The matrix M can be defined as

$$M = \begin{bmatrix} \sum_W (I_m(m_i, n_i))^2 & \sum_W (I_m(m_i, n_i)I_n(m_i, n_i)) \\ \sum_W (I_m(m_i, n_i)I_n(m_i, n_i)) & \sum_W (I_n(m_i, n_i))^2 \end{bmatrix} \qquad (1)$$

where I_m and I_n denote partial derivatives of I with respect to m and n, respectively, and (m_i, n_i) represents pixel position in the window (W). In the third step, a corner response function R is defined to avoid the explicit eigenvalue decomposition of M, written as

$$R = det(M) - k(trace(M))^2 \qquad (2)$$

where k denotes a small positive constant which is set to 0.01 in our experiments empirically, and $det(\cdot)$ and $trace(\cdot)$ are determinant and trace of the matrix, respectively. After

computing the corner response for all pixels, a threshold on the R and the non-maximum suppression is used to get corner points. More details on Harris corner detector can be found in [15].

Fig.1 shows an example of blurred and re-blurred images and their extracted Harris feature points. The re-blurred image (the right one) exhibits less feature points than the blurred image (the left one). The reason is that blur causes image degradation, which leads to feature points reduction. We can also notice that the reduction extent in smooth areas is more obvious than that in texture areas, which proves that feature points can capture image structure changes.
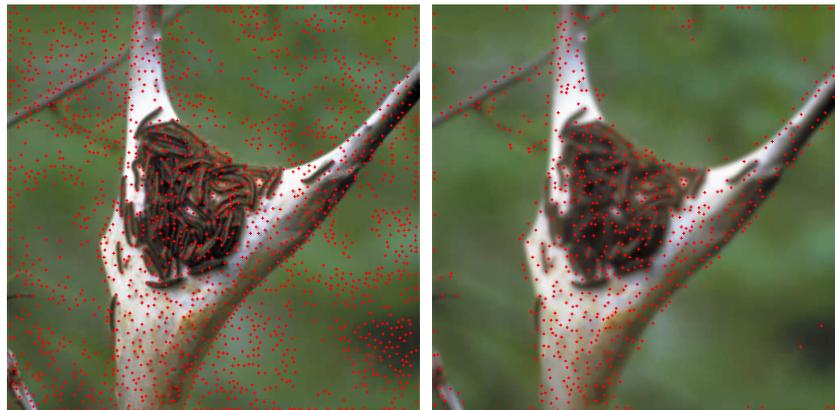

FIGURE 1. An example of blurred and re-blurred images and their extracted Harris feature points

3. **Proposed Method.** Fig.2 shows the flowchart of the proposed image blur assessment method. First, we apply Gaussian blur to the blurred image to obtain the re-blurred image. Then we extract feature points from the blurred and re-blurred images through Harris corner detector, and the the feature point maps are produced. Next, the feature point maps are divided into blocks to compute block-wise quantity maps, then the block-wise quantity similarity map is calculated. At last, a resized visual saliency map is used to pool this similarity map, producing the overall blur score.
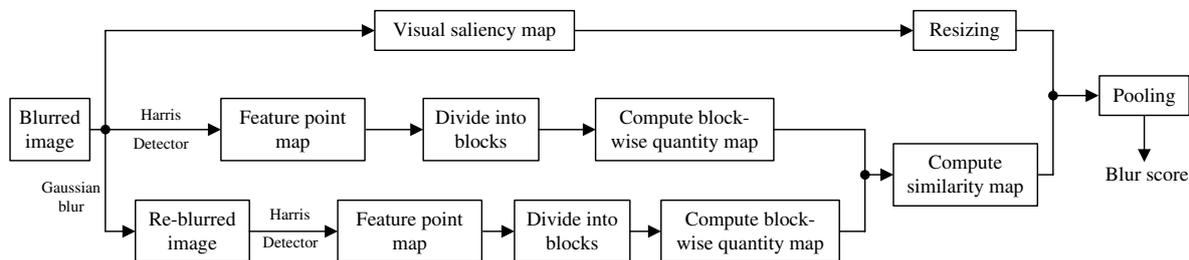

FIGURE 2. Flowchart of the proposed image blur metric

3.1. **Gaussian Blur.** Gaussian blur is widely used to produce a blurred image by reducing the high-frequency components of an image. In this paper, a re-blurred image is produced by applying Gaussian blur to a blurred image with a window size of 3×3 and a standard deviation σ set to 5. While generating the re-blurred images, we conduct the blur operation twice, and we find that for extremely blurred images, further blurring produces little effect.

3.2. **Image Blocking.** The variation of feature points has correlation with geometric structures of image pixels, which means blur extent may differ from different image contents. Instead of directly use all the feature points of a test image to represent its blur extent, we divide the feature points into blocks for better illustration. Given a blurred image I^x and we can get the corresponding re-blurred image I^y, both of them are of size $M \times N$. Through the Harris corner detector we get feature point maps P^x and P^y, respectively. Then they are partitioned into non-overlapping blocks of size $B \times B$, which are denoted by P_{ij}^x and P_{ij}^y, respectively, $i \in \{1, 2 \cdots, E\}$, $j \in \{1, 2 \cdots, T\}$, where $E = \lfloor \frac{M}{B} \rfloor$, $T = \lfloor \frac{N}{B} \rfloor$, $\lfloor \cdot \rfloor$ is the floor operation. Then, we compute the sum of feature points in each block, thus producing the block-wise quantity maps F^x and F^y, respectively, which can be represented as

$$F^x(i,j) = \sum P_{ij}^x \tag{3}$$

$$F^y(i,j) = \sum P_{ij}^y \tag{4}$$

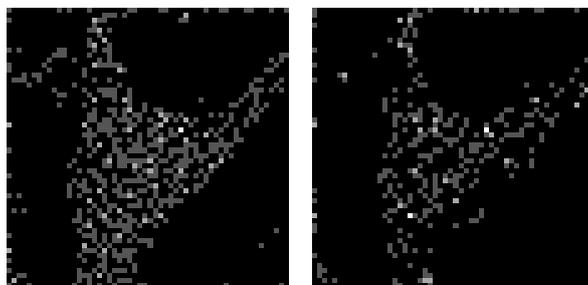where x and y are the blurred and re-blurred images.

FIGURE 3. The block-wise quantity maps of the blurred and re-blurred images in Fig.1

Fig.3 shows the block-wise quantity maps of the blurred and re-blurred images in Fig.1. We can see that the block-wise quantity map of re-blurred image exhibits less feature points, compared to that of the blurred image. Besides, the reduction of quantity varies among different block-pairs, which is caused by different image shape changes.

3.3. **Feature Point Quantity Similarity.** Since we consider to use the difference between blurred image and re-blurred image to represent image quality, the similarity of block-wise quantity maps F^x and F^y is proposed to evaluate the blur extent or relative blur of the test image. With two block-wise quantity maps F^x and F^y, the feature point quantity similarity map is computed as

$$S(i,j) = \frac{2F^x(i,j)F^y(i,j) + C}{[F^x(i,j)]^2 + [F^y(i,j)]^2 + C} \tag{5}$$

where $i \in \{1, 2 \cdots, E\}$, $j \in \{1, 2 \cdots, T\}$, x and y are the blurred and re-blurred images, C is a small constant used to ensure numerical stability. The similarity of feature point quantity maps is computed pixel-wisely, so S serves as a local quality map, which is the indicative of local distortions in the image.

3.4. **Pooling by Visual Saliency.** Visual saliency for quality score pooling has already been used as a weighting method in some previous works [16]. In particular, distortions in textured areas have more impact on the subjective quality than those in smooth areas. The saliency detection algorithms can determine which regions of an image attract the most attention of human eyes automatically.

Fig.4 shows the saliency map detected from the blurred image in Fig.2. We can observe that the detected salient areas correspond to the foreground areas, which contribute more in the perception of blur. With the saliency map of an image, the blur score can be measured by assigning bigger weights to the visually salient areas. As a result, we generate the final image blur score by incorporating visual saliency.
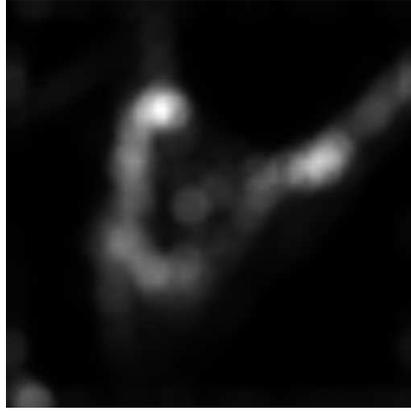

FIGURE 4. The saliency map detected from the blurred image in Fig.1

In this paper, the visual saliency map of the blurred image is first calculated and denoted by $\{V(i,j)\}$, $i \in \{1,2\cdots,M\}$, $j \in \{1,2\cdots,N\}$, Then the saliency map is resized to the size $E \times T$, such that one image block corresponds to one weight. Suppose the resized saliency map is represented by $\{V_R(i,j)\}$, $i \in \{1,2\cdots,E\}$, $j \in \{1,2\cdots,T\}$, the final image blur score is computed as

$$Q = \frac{\sum_{i=1}^{E} \sum_{j=1}^{T} S(i,j)V_R(i,j)}{\sum_{i=1}^{E} \sum_{j=1}^{T} V_R(i,j)}. \tag{6}$$

The proposed method will generate high scores for more blurred images, and the scores will be no greater than 1.

4. Experimental Results and Analysis.

4.1. **Experimental settings.** We evaluate the performance of the proposed method on four public image quality databases, namely LIVE [17], CSIQ [18], TID2008 [19] and TID2013 [20]. The numbers of blurred images in the databases are 145, 150, 100, and 125, respectively. For each image, the subjective quality is measured, which refers to Difference Mean Opinion Score (DMOS) in LIVE and CSIQ, and Mean Opinion Score (MOS) in TID2008 and TID2013.

The size of the blocks is set to 9×9 ($B = 9$) and the Harris corner detector threshold is set to 0.036, which are determined by experiments. In the literatures, many saliency detection models have been proposed. In this paper, we employ the SR model [24], because it can produce slightly better results and is also computationally efficient.

Three commonly used criterions are employed to evaluate the performance of the proposed metric. The first two are the Pearson linear correlation coefficient (PLCC) and the root mean square error (RMSE), which are used to measure the prediction accuracy. Another one is the Spearman rank order correlation coefficient (SROCC), which is used to evaluate the prediction monotonicity. SROCC can be calculated according to the rank

of the scores, while PLCC and RMSE can be computed by applying a nonlinear regression between the subjective scores and the predicted scores. In this paper, we adopt the four-parameter logistic fitting function:

$$f(x) = \frac{\tau_1 - \tau_2}{1 + e^{(x-\tau_3)/\tau_4}} + \tau_2 \qquad (7)$$

where $\tau_1, \tau_2, \tau_3, \tau_4$ are the parameters to be fitted. Typically, an excellent metric exhibits high PLCC and SROCC values, as well as low RMSE value.

4.2. **Performance Evaluation.** In this subsection, we test the performance of the proposed method on the four image quality databases. Only the blurred images in each database are included in the computation.
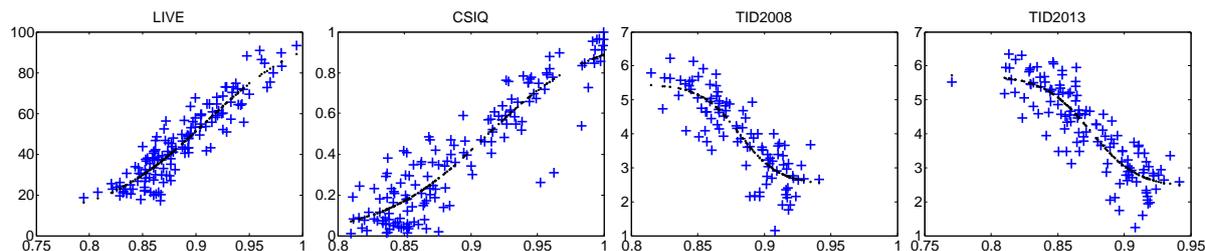

FIGURE 5. Scatter plots of the subjective scores against the predicted blur scores obtained by the proposed metric on four databases. The X-axis denotes the metric score, and Y-axis denotes the subjective score (DMOS for LIVE and CSIQ, MOS for TID2008 and TID2013)

Fig.5 shows the scatter plots of the subjective scores against the predicted scores using our proposed metric on four databases, where test images are represented by the sample points. We can see that the predicted scores have high consistency with subjective evaluations.

We also compare the proposed method against five existing no-reference image sharpness/blur metrics which include Marziliano [11], HP Metric [12], Riem. Metric [13], JNB [7] and Q-Metric [14]. Table 1 summarizes the experimental results of the six blur metrics on the four databases in terms of PLCC, SROCC and RMSE. For each database, the best result is marked in boldface. Note that the performance of one metric may differ from different databases. To provide an overall evaluation, we also compute the weighted average PLCC and SROCC results for each metric over all four databases. The weighted average is based on the size, namely number of blurred images in each database, which means larger size will be assigned bigger weight.

It can be seen from Table 1 that the proposed method achieves the best performance over the four databases, and it outperforms other metrics by a amount of more than about 0.1000 for both PLCC and SROCC values in all databases, which is quite noticeable. For weighted average, our proposed method also achieves the best accuracy and monotonicity, which exhibits really significant improvement. Hence, we can conclude that blur scores predicted by our metric correlate much more consistently with subjective evaluations than all the other blur metrics evaluated.

In order to further illustrate the superiority of the proposed method, we compare it with several general-purpose NR image quality metrics, namely Blind Image Quality Index (BIQI) [21], BLind Image Integrity Notator using DCT Statistics (BLIINDS2) [22] and Blind/Referenceless Image Spatial QUality Evaluator (BRISQUE) [23]. Table 2 lists the simulation results, and we highlight the best result with boldface. It should be noted that BIQI, BLIINDS2 and BRISQUE use the LIVE database to train their quality models, so

TABLE 1. Summary of the experimental results for the proposed method and five existing image blur metrics on four databases

Database	Criterion	Q-Metric [14]	HP [12]	Riem. [13]	Marziliano [11]	JNB [7]	Proposed
LIVE	PLCC	0.6787	0.7402	0.7735	0.8060	0.8160	**0.9187**
	SROCC	0.5482	0.7020	0.7223	0.8043	0.7871	**0.9036**
	RMSE	13.5646	13.1141	11.7071	10.9328	10.6769	**7.2967**
CSIQ	PLCC	0.7219	0.6894	0.8710	0.7969	0.8061	**0.9158**
	SROCC	0.6530	0.7053	0.8415	0.7697	0.7624	**0.8645**
	RMSE	0.1983	0.2076	0.1408	0.1731	0.1696	**0.1151**
TID2008	PLCC	0.3066	0.6286	0.6099	0.7179	0.6931	**0.8460**
	SROCC	0.3276	0.5197	0.5941	0.7252	0.6667	**0.8449**
	RMSE	1.1170	0.9127	0.9300	0.8169	0.8459	**0.6257**
TID2013	PLCC	0.3059	0.7442	0.6643	0.7738	0.7114	**0.8690**
	SROCC	0.3098	0.6861	0.6347	0.7690	0.6902	**0.8663**
	RMSE	1.1880	0.8336	0.9327	0.7904	0.8770	**0.6175**
Weighted	PLCC	0.5300	0.6950	0.7439	0.7787	0.7644	**0.8919**
average	SROCC	0.4787	0.6641	0.7110	0.7706	0.7335	**0.8721**

they are marked by "training images" in the table and not included into comparison for the LIVE database.

TABLE 2. Comparison with the general-purpose no-reference image quality metrics

Database	Criterion	BIQI [21]	BLIINDS2 [22]	BRISQUE [23]	Proposed
LIVE	PLCC	training	training	training	**0.9187**
(145 images)	SROCC	images	images	images	**0.9036**
CSIQ	PLCC	0.8556	0.9102	**0.9279**	0.9158
(150 images)	SROCC	0.7713	0.8915	**0.9033**	0.8645
TID2008	PLCC	0.7550	0.8415	0.8043	**0.8460**
(100 images)	SROCC	0.7468	0.8388	0.7990	**0.8449**
TID2013	PLCC	0.7819	0.8580	0.8240	**0.8690**
(125 images)	SROCC	0.7642	0.8557	0.8134	**0.8663**

It can be observed from the table that the proposed method outperforms all the compared general-purpose NR image quality metrics by the best overall performance on four databases. Although BRISQUE performs the best in CSIQ, the performances on the rest databases are not very competitive. Compared with these general-purpose NR image quality metrics, our metric has the advantage of less computation cost for no training model procedure. Besides, our proposed method exhibits a comparable well performance.

5. **Conclusions.** Blur is a key factor in perception of image quality. Based on the observation that blur distortion leads to the shape of images and this kind of shape changes can be represented using feature points variations, we have proposed a novel image blur metric based on feature points. In this paper, we first extract feature points from the blurred image and re-blurred image, then the two feature point maps are divided into blocks to generate block-wise quantity map respectively. Later, the block-wise quantity maps are combined to compute the feature point quantity similarity map. Finally, an overall blur score is achieved by pooling this similarity map with a visual saliency map.

We have done extensive experiments on public image quality databases. The experimental results demonstrate that the proposed method can produce blur scores highly consistent with human perception. We have also compared the proposed method with representative image blur metrics as well as several general-purpose no-reference image quality metrics, and the results demonstrate the superiority of our method.

REFERENCES

[1] D. M. Chandler, Seven challenges in image quality assessment: past, present, and future research, *ISRN Signal Process*, vol. 2013, Article ID. 905685, pp.1-53, 2013.

[2] J. S. Qian, D. Wu, L. D. Li, D. Q. Cheng, and X. S. Wang, Image quality assessment based on multi-scale representation of structure, *Digital Signal Processing*, vol. 33, pp. 125-133, 2014.

[3] J. J. Wu, W. S. Lin, G. M. Shi, and A. M. Liu, Reduced-reference image quality assessment with visual information fidelity, *IEEE Trans. on Multimedia*, vol. 15, no. 7, pp. 1700-1705, 2013.

[4] L. D. Li, H. C. Zhu, G. B. Yang, and J. S. Qian, Referenceless measure of blocking artifacts by Tchebichef kernel analysis, *IEEE Signal Process. Letters*, vol. 21, no. 1, pp. 122-125, 2014.

[5] L. D. Li, W. S. Lin, and H. C. Zhu, Learning structural regularity for evaluating blocking artifacts in JPEG images, *IEEE Signal Processing Letters*, vol. 21, no. 8, pp. 918-922, 2014.

[6] W. Zhang, L. D. Li, H. C. Zhu, D. Q Cheng, S. C Chu, and J. F Roddick, No-reference quality metric of blocking artifacts based on orthogonal moments, *Journal of Information Hiding and Multimedia Signal Processing*, vol. 5, no. 4, pp. 701-708, 2014.

[7] R. Ferzli and L. J. Karam, A no-reference objective image sharpness metric based on the notion of just noticeable blur (JNB), *IEEE Trans. Image Process*, vol. 18, no. 4, pp. 717-728, 2009.

[8] G. Cao, Y. Zhao, and R. R. Ni, Edge-based blur metric for tamper detection, *Journal of Information Hiding and Multimedia Signal Processing*, vol. 1, no. 1, pp. 20-27, 2010.

[9] H. T. Liu, N. Klomp, and I. Heynderickx, A no-reference metric for perceived ringing artifacts in images, *IEEE Trans. Circuits Syst. Video*, vol. 20, no. 4, pp. 529-539, 2010.

[10] W. F. Xue, X. Q. Mou, L. Zhang, A. C. Bovik and X. C. Feng, Blind image quality assessment using joint statistics of gradient magnitude and Laplacian features, *IEEE Trans. Image Process*, vol. 23, no. 11, pp. 4850-4862, 2014.

[11] P. Marziliano, F. Dufaux, S. Winkler, and T. Ebrahimi, Perceptual blur and ringing metrics: application to JPEG2000, *Signal Processing: Image Communication*, vol. 19, no. 2, pp. 163-172, 2004.

[12] D. Shaked and I. Tastl, Sharpness measure: Towards automatic image enhancement, *Proc. of IEEE Int. Conf. Image Process*, vol. 1, pp. 937-940, 2005.

[13] R. Ferzli and L. J. Karam, A no-reference objective image sharpness metric using Riemannian tensor, *Third International Workshop on Video Processing and Quality Metrics for Consumer Electronics VPQM-07*, Scottsdale, Arizona, 2007.

[14] X. Zhu and P. Milanfar, Automatic parameter selection for denoising algorithms using a no-reference measure of image content, *IEEE Trans. Image Process*, vol. 19, no. 12, pp. 3116-3132, 2010.

[15] C. Harris and M. J. Stephens, A combined corner and edge detector, *Proc. of Alvey Vision Conf.*, pp. 147-152, Manchester, U.K., 1988.

[16] A. K. Moorthy and A. C. Bovik, Visual importance pooling for image quality assessment, *IEEE J. Sel. Topics Signal Process.*, vol. 3, no. 2, pp. 193-201, 2009.

[17] H. R. Sheikh, M. F. Sabir, and A. C. Bovik, A statistical evaluation of recent full reference image quality assessment algorithms, *IEEE Trans. Image Process.*, vol. 15, no. 11, pp. 3440-3451, 2006.

[18] E. C. Larson and D. M. Chandler, Most apparent distortion: Full reference image quality assessment and the role of strategy, *J. Electronic Imaging*, vol. 19, no. 1, pp.011006:1-21, 2010.

[19] N. Ponomarenko, V. Lukin, A. Zelensky, K. Egiazarian, M. Carli, and F. Battisti, TID2008-a database for evaluation of full-reference visual quality assessment metrics, *Advances of Modern Radio electronics*, vol. 10, no. 4, pp. 30-45, 2009.

[20] N. Ponomarenko, O. Ieremeiev, V. Lukin, K. Egiazarian, L. Jin, J. Astola, B. Vozel, K. Chehdi, M. Carli, F. Battisti, and C. J Kuo, Color image database TID2013: peculiarities and preliminary results, *Proc. of European Workshop on Visual Information Processing*, pp. 106-111, 2013.

[21] A. K. Moorthy and A. C. Bovik, A two-step framework for constructing blind image quality indices, *IEEE Signal Process. Letters*, vol. 17, no. 5, pp. 513-516, 2010.

[22] M. A. Saad and A. C. Bovik, Blind image quality assessment: a natural scene statistics approach in the DCT domain, *IEEE Trans. Image Process.*, vol. 21, no. 8, pp. 3339-3352, 2012.

[23] A. Mittal, A. K. Moorthy, and A. C. Bovik, No-reference image quality assessment in the spatial domain, *IEEE Trans. Image Process.*, vol. 21, no. 12, pp. 4695-4708, 2012.

[24] X. D. Hou and L. Q. Zhang, Saliency detection: a spectral residual approach, *Proc. of IEEE Conference on Computer Vision and Pattern Recognition (CVPR)*, pp. 1-8, 2007.